Mechanism of *n*-butane skeletal isomerization on H-mordenite and Pt/H-mordenite

*Matthew J. Wulfers, Friederike C. Jentoft**

School of Chemical, Biological and Materials Engineering, University of Oklahoma, Norman, OK 73019-1004, USA; corresponding author: fcjentoft@ou.edu

Abstract

Kinetics and isotope labeling experiments were used to investigate the reaction pathways of *n*-butane on H-mordenite and Pt/H-mordenite at atmospheric pressure and temperatures of 543 to 583 K. Butenes, either formed on the catalyst or present in the feed, controlled the relative rates of mono- and bimolecular reaction pathways. The true activation energy for isobutane formation was found to be 120–134 kJ/mol. The reaction order for isobutane formation with respect to *n*-butene on Pt/H-mordenite was 1.0-1.2, consistent with a predominately monomolecular route of formation. An order close to 2 for disproportionation products indicated a bimolecular route of formation. An increase of the butene concentration from less than 20 ppm to about 120 ppm greatly increased the rate of bimolecular skeletal isomerization, as determined from conversion of 1,4-$^{13}C_2$-*n*-butane. The findings explain how reaction conditions affect product selectivity and clarify the controversy around butane isomerization on solid acids.

Keywords: Zeolite; MOR; Intramolecular; beta-Scission; Binomial Distribution; Equilibrium; Dual-Functional; Isotopic Scrambling; Olefins

1 Introduction

Skeletal isomerization of *n*-butane is of interest, both with respect to commercial application and with respect to the fundamental understanding of reaction mechanisms in acid catalysis. The isomerization product, isobutane, is used in large quantities for C4 alkylation and production of methyl *tert*-butyl ether and ethyl *tert*-butyl ether via isobutene [1,2]. Isobutane can be produced from its less valuable skeletal isomer, *n*-butane, via acid-catalyzed skeletal isomerization. The mechanistic details of this reaction have been the subject of intense debate in the open literature [3-5].

In contrast to the heavily debated mechanism of *n*-butane isomerization, skeletal isomerization of paraffins with five or more carbon atoms is known to occur via a monomolecular reaction pathway [6,7]. Butane isomerization is thought to be a special case, and it has been claimed that monomolecular skeletal isomerization of butane on solid acids does not occur [8,9], or occurs very slowly [10] or with great difficulty [11], or is not the main isomerization pathway [12,13]. However, numerous solid acids catalyze butane skeletal isomerization at significant rates, implying that either the above claims are incorrect or that an alternative reaction pathway exists. Thus far, many have claimed that a bimolecular (i.e. intermolecular) reaction pathway is responsible, which would involve formation of C8 intermediates from two C4 entities, rearrangement of the C8 intermediate, beta-scission of the C8 intermediate, and further hydride transfer or hydrogenation to form either isobutane or side products [12].

Arguments against the monomolecular butane isomerization pathway originate in the mineral acid catalysis literature. Brouwer [14] found that the skeletal isomer of *n*-butane was not formed in the superacid HF-SbF_5 under conditions in which the skeletal isomer of *n*-pentane formed readily. Intramolecular carbon scrambling in *n*-butane, however, occurred at rates similar to those

of *n*-pentane skeletal isomerization [14,15]. The contrasting behavior can be explained by the postulated transition states and intermediates. *n*-Alkanes with at least five carbon atoms isomerize via a classical cyclopropane ring structure that opens to a secondary carbenium ion of the skeletal isomer. This monomolecular pathway is accepted for both homogenous and heterogeneous catalysts [16]. In the case of butane or butene conversion in mineral acids, opening the cyclopropane ring to form the skeletal isomer results in a primary carbenium ion [17], which is the main argument against a monomolecular skeletal isomerization pathway for these species [13]. Hence, the butane isomerization activity of sulfated zirconia, chlorided alumina, heteropolyacids, and zeolites [16] is often (but not always) ascribed to bimolecular dimerization-cracking pathways, which circumvent the prohibitive energetic requirements of the monomolecular pathway. One large drawback of such bimolecular pathways is that they are not selective to isobutane; the so-called disproportionation products propane and pentanes are also formed at significant rates [18] through cleavage of C8 intermediates.

The zeolite H-mordenite is a catalyst that has been investigated extensively as a butane isomerization catalyst, yet no consensus has evolved on the contributions of mono- and bimolecular reaction pathways to the final product distribution. Experimental evidence suggesting dominance of bimolecular pathways includes: intermolecular carbon-13 scrambling in products formed from 1-^{13}C-*n*-butane [19] and 1-^{13}C-isobutane [20], production of propane and pentane side products [13,21], isobutane reaction orders with respect to *n*-butane of close to 2 [8,21], and a product distribution similar to that from isooctane [22]. Evidence of a significant contribution of a monomolecular skeletal isomerization pathway includes: isobutane reaction orders with respect to *n*-butane of 1.17 [23] and 1 [21], and the inability to model isobutane formation using only a first or second order kinetic model [24]. Additionally, some investigators reported that selectivity

to isomerization or disproportionation products is affected by process conditions such as temperature [13], concentration of acid sites [13,23], conversion [13], reactant partial pressure [13,24], and presence of H_2 [21]; however, a consistent explanation for these dependencies does not exist.

One variable that has been investigated to some extent, but has not been linked to specific reaction pathways or product selectivities, is the concentration of alkenes. Pines and Wackher [25], who worked with an $AlCl_3$/HCl catalyst, reported a promoting effect of alkenes on *n*-butane isomerization. Butane conversion on the zeolite H-mordenite can also be promoted by addition of alkenes; Fogash et al. observed that H-mordenite was completely inactive for *n*-butane [26] or isobutane [27] conversion in the absence of butene in the feed, but was very active when as little as 55 ppm of butene was co-fed. The effect of alkenes is not specific to butene; Engelhardt [28] found that *n*-butane conversion on H-mordenite could be enhanced by addition of ethene, propene, or isobutene to the feed. The data shows an increase in selectivity to disproportionation products upon addition of any alkene, but this effect was not discussed by the author. Similar observations have been made with sulfated zirconia; alkenes reportedly promote conversion of *n*-butane [29-33] and deactivation [26,30]. Intermolecular isotope scrambling in isobutane formed from 1,4-$^{13}C_2$-*n*-butane can be controlled by inclusion of platinum on sulfated zirconia and H_2 in the feed [34,35]. Inclusion of platinum and H_2 caused isobutane to retain the same number of isotopes as the feed, which is indicative of a monomolecular isomerization pathway, whereas the absence of platinum and H_2 resulted in significant intermolecular isotope scrambling. The authors hypothesized that the butene concentration was low in experiments with platinum and H_2, which was considered as not conducive to the bimolecular pathway, but the butene concentration was not

reported. In fact, effluent alkene concentrations are typically not documented; a rare exception is the work by Weisz and Swegler on hexane isomerization [36].

The goal of this investigation was to determine the contributions of monomolecular and bimolecular isomerization and disproportionation pathways on H-mordenite and be able to describe the process variable(s) that control their relative rates. This knowledge would allow one to predict changes in rate and selectivity with changing reaction conditions and possibly design processes in which the selectivity to a desired product can be tuned based on a physical understanding of the reaction chemistry. In theory, the products of monomolecular and bimolecular reaction pathways should be distinguishable by kinetics parameters, such as reaction order and activation energy, and the extent of intermolecular isotope scrambling. If propane, pentanes, and isobutane are all produced through similar bimolecular pathways, their kinetics parameters and experimentally determined isotope distributions may be similar. Isotope distributions in products of a bimolecular pathway should always be binomial, whereas the possibility exists for isobutane to retain the same number of isotopes as the feed if it is formed through a monomolecular pathway.

2 Materials and methods

2.1 Materials

NH_4-mordenite (Lot 32125-99) and Pt/H-mordenite (Lot 33407-1, not pre-reduced by the manufacturer and Lot 33436-24, pre-reduced) zeolites were received from UOP, a Honeywell company. The Si/Al ratio of all samples was 9.1, specified by ICP-AES performed by the manufacturer. Platinum had been introduced by the incipient wetness method using hexachloroplatinic acid as the precursor; the platinum content was 0.328 wt %, also specified by

ICP-AES. Calcination of the NH_4-mordenite was performed in a horizontal furnace. A quartz boat containing 1.5 g of catalyst was placed inside a 2.3 cm ID quartz tube, which was placed inside the furnace under a 100 ml min^{-1} flow of air (Airgas, zero grade). The temperature was first increased at 2 K min^{-1} to 423 K, held for 1 h, and then increased at 5 K min^{-1} to 873 K and held for 2 h.

Reactant gases were of the following purities: *n*-butane (Matheson, 99.99 %) containing 14 ppm isobutane and < 1 ppm propene impurities, and 1,4-$^{13}C_2$-*n*-butane (Isotec Inc., specified as 99.7 % gas purity and 99 % isotope purity) with 5200 ppm ethane and 1200 ppm 1-butene impurities as quantified by in-house GC analysis. Other gases were N_2 (Airgas, UHP 99.999 %), O_2 (Airgas, UHP 99.994 %), H_2 (Airgas, UHP 99.999 %), and helium (Airgas, UHP 99.999 %). All inorganic gases were passed through moisture traps (Agilent, MT400-2 for N_2, O_2, and H_2; Restek for helium), and N_2 was also passed through an O_2 trap (Chromres, Model 1000).

2.2 Test apparatus and pretreatment conditions

All catalytic experiments were performed at atmospheric pressure in down-flow packed-bed reactors. Zeolite powder was placed in a borosilicate glass tube (5.5 mm ID) between two pieces of quartz wool. The tube was heated by an electrically powered furnace, and the temperature was controlled by an Omega CN3251 controller using a K-type thermocouple placed in a well at the center of the furnace's isothermal zone. The pressure drop through the catalyst bed was monitored, and was less than 0.5 psi during all experiments. Quantification of products was performed by a gas chromatograph (Varian 3800 GC) using a Fused Silica PLOT column (Chrompack, 0.32 mm ID x 60 m) for separation and both thermal conductivity and flame ionization detectors connected in series. In experiments with 1,4-$^{13}C_2$-*n*-butane as reactant, a gas chromatograph equipped with a mass spectrometer detector (GC-MS, Agilent 5975E) was used to determine the isotope

distribution in individual products. The electron impact ionization source in the GC-MS was operated at 70 eV, and products were separated using a GS-Gaspro PLOT column (Agilent, 0.32 mm ID x 60 m). Splitless injections were performed on the GC-MS in all cases except when Pt/H-mordenite was used without an alkene trap, in which case a split ratio of 5:1 was used. Mass flow controllers (Bronkhorst) were used to control gas flow rates, and gas transfer lines were heated to a temperature of 343 K.

2.3 Pretreatment of catalysts

Pretreatment of H-mordenite began by raising the temperature at 5 K min^{-1} to 673 K in a 30 ml min^{-1} (NTP) flow of synthetic air and continued with sequential 0.5 h treatments in synthetic air, N_2, and H_2. Pretreatment of Pt/H-mordenite began by heating at 5 K min^{-1} to 403 K in a 30 ml min^{-1} flow of N_2 and holding the temperature for 4 h. The temperature was then increased at 5 K min^{-1} to the final reduction temperature in a flow of H_2 and held for 4 h. The final reduction temperature and H_2 flow rate were 560 K and 30 ml min^{-1}, except in experiments with varying space time, in which a final reduction temperature and H_2 flow rate of 573 K and 50 ml min^{-1} were used.

2.4 Conversion of *n*-butane on H-mordenite with controlled concentration of *n*-butenes in the feed

An experiment was performed with two reactors placed in series, whereby the first reactor was used to control the concentration of *n*-butenes in the feed to the second reactor. The first reactor was an HVC-VUV environmental chamber from Harrick Scientific (which is commonly used for in situ diffuse reflectance spectroscopy) and contained 70 mg of a 1 wt % Pt/SiO_2 catalyst (preparation details and characterization of the Pt/SiO_2 can be found in Ref. 37). The Pt/SiO_2 catalyst was reduced in the environmental chamber at a temperature of 548 K in H_2 flowing at 30

ml min^{-1} for 1.5 h and was then cooled to the desired operating temperature. The flow to the chamber consisted of 3 ml min^{-1} of *n*-butane and 12 ml min^{-1} of helium, and was admixed with 15 ml min^{-1} H_2 between the first and second reactors. A temperature of 323 K was used in the first reactor to keep the concentration of butenes below the detection limit of the GC, which was about 1 ppm, and a temperature of 433 K was used to control the butene concentration at 18 ppm. The second reactor was the apparatus described in Section 2.2, which held 87 mg of H-mordenite.

2.5 Measurement of product formation rates on H-mordenite and Pt/H-mordenite over a range of temperatures, *n*-butane partial pressures, and H_2 partial pressures

Experiments were performed using the apparatus described in Section 2.2. Either 82 mg of H-mordenite or 80 mg of Pt/H-mordenite (Lot 33407-1) was used as the catalyst. Product formation rates were measured over a range of temperatures (543–583 K, 10 K increments), *n*-butane partial pressures (3.3–13.3 kPa, 3.3 kPa increments), and H_2 partial pressures (30–90 kPa, 20 kPa increments). The total conversion of *n*-butane was in the range of what is considered to be differential, not exceeding 1.7 % on H-mordenite or 2.6 % on Pt/H-mordenite. Because conversions were low, a product-based conversion *X* defined in Eq. 1 was used throughout the manuscript.

$$X\,\% = \frac{F_{C,prod}}{F_{C,total}} \times 100 \qquad (1)$$

Where $F_{C,prod}$ is the flow rate of carbon atoms from product molecules in the reactor effluent stream (i.e. everything except *n*-butane) and $F_{C,total}$ is the total flow rate of carbon atoms in the reactor effluent stream (i.e. includes *n*-butane). Selectivities are reported as molar selectivities and were calculated according to Eq. 2:

$$S_x\ \% = \frac{F_x}{F_t} \times 100 \tag{2}$$

S_x is the selectivity for an individual product in percent, F_x is the molar flow rate of the individual product, and F_t is molar flow rate of all gas phase products.

Conversion of *n*-butane on both catalysts began at conditions of 543 K, 3.3 kPa *n*-butane, and 90 kPa H_2. Helium was used to balance to atmospheric pressure. After taking four GC measurements over a duration of about 1 h, the temperature was increased by 10 K and four measurements were again taken. This procedure was repeated until measurements had been taken over the specified range of temperatures. The temperature was then lowered to 543 K and four measurements were taken at the initial set of conditions to determine if deactivation had occurred. The partial pressure of *n*-butane was then increased by 3.3 kPa while holding the partial pressure of H_2 constant and the procedure was repeated. After taking measurements at the four *n*-butane partial pressures of interest, the partial pressure of H_2 was lowered by 20 kPa and the procedure was repeated. This protocol was used to gather rate data under all conditions of interest or until deactivation was apparent from time on stream data. An example of the data generated with increasing temperature is shown in Figure S1 in the supporting information.

2.6 Measurement of product formation rates on Pt/H-mordenite at various space times

Experiments were performed using the apparatus described in Section 2.2. A minor deviation was that Pt/H-mordenite powder (Lot 33436-24) was mixed with 1.0 mm diameter quartz beads in a 3:2 mass ratio and supported in a quartz tube (12 mm ID) by a quartz frit. Four catalyst loadings between 0.10 g and 1.00 g were used. Reactions were performed at a temperature of 573 K applying a total gas flow rate of 50 ml min^{-1}, with the gas mixture composed of 10 kPa *n*-butane, 50 kPa H_2, and helium for balance.

2.7 Collection of data during conversion of 1,4-$^{13}C_2$-*n*-butane

Conversion of 1,4-$^{13}C_2$-*n*-butane was performed on 81-87 mg of H-mordenite or Pt/H-mordenite (Lot 33407-1) either with or without purification of the feed. For experiments in which the feed was purified, the feed stream passed through a separate quartz tube containing a bed of HY zeolite (190-200 mg, Zeolyst, Si/Al = 2.5), which served as an alkene trap, before reaching the reactor that contained mordenite. The HY zeolite was pretreated by heating to a temperature of 473 K in the starting gas flow (either synthetic air for H-mordenite or N_2 for Pt/H-mordenite) and was held at this temperature for 1 h before heating of the mordenite began. At the end of the mordenite pretreatment, the HY zeolite was cooled to ambient temperature and the temperature of the reactor containing the mordenite was set to 573 K. The reactant gas mixture was then admitted to the reactor. A flow of 21 ml min^{-1} H_2, 6 ml min^{-1} helium, and 3 ml min^{-1} 1,4-$^{13}C_2$-*n*-butane was used as a standard composition except for the experiment employing Pt/H-mordenite without feed purification, in which case the gas mixture was composed of 27 ml min^{-1} H_2 and 3 ml min^{-1} 1,4-$^{13}C_2$-*n*-butane. In experiments without feed purification, measurements by online GC-FID and GC-MS were started 3 min after hydrocarbon flow to the reactor had begun. In experiments with feed purification, the first injection was taken 6.5 min after hydrocarbon flow to the reactor had begun. Conversion of *n*-butane to gas phase products was less than 4 % in all cases.

3 Results

3.1 Effect of *n*-butenes in the feed on product formation rates

Figure 1 demonstrates the dramatic effect that *n*-butenes have on the rate of *n*-butane conversion. A butene-free feed was used initially, and there was no conversion of *n*-butane to gas phase products. After 75 min on stream, 18 ppm of *n*-butenes were added to the feed, resulting in

significant conversion of *n*-butane. The concentration of products in the reactor effluent is shown in Figure 1 instead of the rate to illustrate the magnitude of the effect of the *n*-butenes on gas phase product formation. The isobutane concentration reached 415 ppm and the concentrations of propane and pentanes (*n*-pentane and 2-methylbutane) were between 60 and 80 ppm. The concentration of *n*-butenes in the effluent stream was 1-3 ppm. A slight decrease in product concentrations with time was observed starting at about 100 min on stream, that is, soon after butenes were introduced and conversion was stimulated.

Initially unknown to the experimenters, the commercial 1,4-$^{13}C_2$-*n*-butane also contained butene, which was present as an impurity in the as-purchased commercial product. Diluted to a partial pressure of 10 kPa, the isotopically labeled feed contained 120 ppm of 1-butene. Thus, product formation rates and selectivities differed on catalysts, especially H-mordenite, used with and without a bed of HY zeolite acting as a butene adsorbent (see rates and selectivities of main products in Table 1 or all products in Table S5 in the supporting information). Without the alkene trap (that is, with 120 ppm of 1-butene in the feed) the rate of isobutane formation on H-mordenite was 1770 μmol g^{-1} h^{-1} and the isobutane selectivity was 60 %. With an alkene trap, the rate of isobutane formation was 765 umol g^{-1} h^{-1} and the isobutane selectivity was 78 %. Both rate measurements are higher than when an unlabeled feed was used, and considering that butenes increase the rate of *n*-butane conversion, it is possible that the alkene trap was only partially effective.

3.2 Comparison of *n*-butene effluent concentrations with equilibrium concentrations

When unlabeled *n*-butane was used, the measured concentrations of *n*-butenes (i.e., 1-butene, *trans*-2-butene, and *cis*-2-butene) in the reactor effluent were within 10-34 % (generally 10-20 %) of the calculated equilibrium concentrations over the entire range of conditions on Pt/H-mordenite

and at high H_2 partial pressures on H-mordenite (see the concentration of *trans*-2-butene in Figure 2 and an analysis over a wider range of reaction conditions in Section S2 of the supporting information). When Pt/H-mordenite was the catalyst, the effluent butene concentrations were close to equilibrium at H_2 partial pressures of 50, 70, and 90 kPa. When H-mordenite was used, the concentration of *n*-butenes deviated significantly from the calculated equilibrium concentration at low H_2 partial pressures, but was close to equilibrium at a H_2 partial pressure of 90 kPa. The three *n*-butene isomers were always present in ratios expected from thermodynamics.

When isotopically labeled *n*-butane was used, the *n*-butene concentration was slightly below the calculated equilibrium concentration in experiments on Pt/H-mordenite both with and without the alkene trap, and were within 2 ppm of concentrations measured with an unlabeled feed (Table 1). On H-mordenite, the concentration of *n*-butenes was always higher than the calculated equilibrium concentration. When an alkene trap was used, the concentration was 1 ppm higher, and when the alkene trap was not used, the measured concentration of 32 ppm was twice the calculated equilibrium concentration of 16 ppm (Table 1).

3.3 Trends in product formation rates and selectivities with changing reaction conditions or space time

The product formed with the highest rate and highest selectivity under all reaction conditions was isobutane (Figure 3 and Table 1). Propane and pentanes were the most significant side products, with the propane to pentanes ratio being always larger than 1. Pentanes are taken to be representative of the bimolecular pathway throughout the manuscript because propane can also be produced on platinum via hydrogenolysis (although even without platinum, the propane/pentanes ratio was slightly greater than 1). Methane, ethane, ethene, propene, and hexanes (i.e. *n*-hexane, 2-methylpentane, and 3-methylpentane) were minor products (see Table S5 in the Supporting

Information for a complete product distribution). Butenes (including some isobutene at higher conversions) were detected in the product stream even when the unlabeled feed, which did not contain any butene as an impurity, was used.

In kinetics experiments with unlabeled *n*-butane, the rate of product formation increased with increasing temperature, increasing *n*-butane partial pressure, and decreasing H_2 partial pressure (Figure 3). Concurrent with this increase in overall rate (and thus conversion) was a decrease in selectivity to isobutane and an increase in selectivity to side products, represented by pentanes in Figure 3. The only parameter that did not cause a drastic change in selectivity was the space time, which caused a decrease in isobutane selectivity of only 3.1 % as conversion increased from 0.9 to 8.0 %.

3.4 Conversion of 1,4-$^{13}C_2$-*n*-butane on H-mordenite

The rates of product formation on H-mordenite using a 1,4-$^{13}C_2$-*n*-butane feed containing 120 ppm of 1-butene as an impurity were significantly higher than the rates observed with an unlabeled, butene-free feed (Table 1). The selectivity to isobutane of 60 % was also significantly lower than observed with the unlabeled feed. The concentration of *n*-butenes in the effluent stream was 32 ppm, which is higher than the equilibrium concentration of 16 ppm.

When 1,4-$^{13}C_2$-*n*-butane was passed through an alkene trap before reaching the catalyst bed, the rate of isobutane formation was 765 μmol g^{-1} h^{-1}, much lower than the rate of 1770 μmol g^{-1} h^{-1} obtained with the non-purified feed. The rates of propane and pentane formation were also lower with the purified feed. The selectivity to isobutane increased, from 60 % with the non-purified feed to 78 % with the purified feed. The concentration of *n*-butenes in the reactor effluent was 17 ppm.

Significant intermolecular isotope scrambling was seen in all products when the feed was not purified. Isobutane molecules with two carbon-13 atoms accounted for 49 % of the isobutane

formed, whereas 37.5 % is expected in a binomial distribution (Table 2). 2-Methylbutane and *n*-pentane, which are products that can only come from a bimolecular pathway, contained 2 or 3 carbon-13 isotopes in 34–36 % of the product, whereas 37.5 % constitutes a binomial distribution.

With a purified feed, 70 % of isobutane molecules retained two carbon-13 atoms (Table 2). The fractions of propane molecules with one and two carbon-13 atoms were 45 % and 38 %, respectively, whereas 37.5 % is expected in a binomial distribution. Both *n*-pentane and 2-methylpentane also had a slightly larger fraction of species with two and three carbon-13 atoms than expected in a binomial distribution (i.e., 37.5%). One should note that the concentrations of the disproportionation products propane, *n*-pentane, and 2-methylbutane were low (115 ppm for propane, < 55 ppm for each pentane), and measurement of their mass distribution relied on data near the detection limits of the GC-MS.

3.5 Conversion of 1,4-$^{13}C_2$-*n*-butane on Pt/H-mordenite

Conversion of 1,4-$^{13}C_2$-*n*-butane with 120 ppm of 1-butene on Pt/H-mordenite resulted in product formation rates, selectivities, and isotope distributions that differed considerably from those produced on the platinum-free H-mordenite. The rate of isobutane formation was only 375 μmol g^{-1} h^{-1}, and the selectivity to isobutane was 77 %, which was 17 % higher than on H-mordenite. The isotope distribution in isobutane also changed considerably; the fraction with two carbon-13 isotopes was 72 %. The concentrations of propane and pentane were too low to measure a reliable mass spectrum by GC-MS.

In contrast to what was observed on H-mordenite, product formation rates and selectivities on Pt/H-mordenite using purified and non-purified 1,4-$^{13}C_2$-*n*-butane were similar. The selectivity to isobutane of 83 % on Pt/H-mordenite with the alkene trap was the highest measured under any set of conditions, but was only marginally higher than the 77 % selectivity observed with a non-

purified feed. Purification of the feed also resulted in 81 % of isobutane molecules retaining two carbon-13 isotopes. This percentage was the largest observed, and coincided with the maximum measured selectivity to isobutane. The percentage of isobutane species containing a number of carbon-13 atoms other than two did not seem to follow a pattern. The low concentration of propane and pentanes again prohibited an accurate measurement of their isotope distributions.

4 Discussion

4.1 Impact of butenes in the feed on product formation rates and selectivities

Figure 1 shows that H-mordenite did not convert *n*-butane at a temperature of 473 K in the absence of butenes in the feed, but became active after introduction of 18 ppm of *n*-butene. This behavior indicates that *n*-butane cannot be protonated by the Brønsted acid sites of H-mordenite (at a temperature of 473 K), and is in agreement with the results of Fogash et al. [26]. The isobutane to butene ratio of ~20 demonstrates that each butene initiates multiple turnovers; *n*-butane molecules are probably activated through hydride transfer. A new observation is the net consumption of *n*-butene, which was evident through an *n*-butene concentration in the effluent stream of 1–3 ppm. Possible explanations for the disappearance of butenes are i) an approach to the chemical equilibrium concentration, which would be 0.1 ppm of *n*-butene under the applied conditions, through hydrogenation to *n*-butane on acid sites [38] or ii) formation of carbonaceous deposits, consistent with the observed slight decline in conversion also seen by others [26] and the reported propensity of alkenes to react and form stable cyclic surface species [39].

At temperatures of about 523 K and above, the zeolite is able to catalyze skeletal isomerization in the absence of alkenes in the feed. However, addition of butene to the feed still caused an increase in product formation rates and also a decrease in selectivity to isobutane. The

observation is exemplified by experiments in which 1,4-$^{13}C_2$-*n*-butane was used as the reactant. Diluted to a partial pressure of 10 kPa for the hydrocarbon, the feed contained 120 ppm of 1-butene. When H-mordenite was used without an alkene trap, there was obviously an *n*-butene gradient from 120 to 32 ppm through the catalyst bed. The *n*-butene concentration in the effluent was 17 ppm when the feed was purified, which is close to the equilibrium value of 16 ppm and suggests that the trap removed a considerable amount of butene from the feed. The two scenarios of high and low butene concentration resulted in product formation rates and selectivities that were drastically different. Without the trap, isobutane formation rates were slightly more than three times larger than rates measured when an alkene-free, unlabeled *n*-butane feed was used. Pentane formation rates were ~8 times greater than when an unlabeled feed was used. Thus, the rate of formation of disproportionation products was affected more by butenes than the rate of formation of the isomerization product, and the selectivity to isobutane of 60 % with the labeled feed was thus the lowest measured in any scenario. When the alkene trap was used, the isobutane formation rate was only marginally higher than the rate with unlabeled feed, and the selectivity of 78 % was only 3 percentage points lower than when an unlabeled feed was used. One might argue that because butene enhances product formation rates, secondary reactions of isobutane will become prominent and alter the selectivity. However, the space time data in Figure 3 clarifies that the product selectivity is only a weak function of conversion, and the low selectivity to isobutane cannot be attributed to secondary reactions. Thus, butenes in the feed are linked to high product formation rates, low selectivity to isobutane, and an increase in selectivity to the disproportionation products propane and pentane.

4.2 Evidence for equilibration of *n*-butane, *n*-butene, and H_2

Because alkenes have a dramatic effect on catalytic performance, knowing their actual concentration in the catalyst bed is compulsory. Moreover, it is important to realize that under conditions of differential conversion of *n*-butane, there may still be a considerable axial alkene gradient in a plug flow reactor that must be accounted for in a kinetics analysis.

H-form zeolites can catalyze hydrogenation and dehydrogenation of alkanes and alkenes [38], but platinum is known to be more effective [40]. Hence, it is conceivable that, especially on Pt/H-mordenite, an equilibrium between *n*-butane, *n*-butenes, and H_2 (Eq. 3) may be reached inside the reactor.

$$n\text{-}C_4H_{10}(g) \leftrightharpoons n\text{-}C_4H_8(g) + H_2(g) \quad (3)$$

All evidence points towards rapid equilibration on Pt/H-mordenite. A first indication is the measured butene concentrations, shown in Figure 2 for experiments with unlabeled *n*-butane and Table 1 for 1,4-$^{13}C_2$-*n*-butane, which were generally within 10-20 % of the calculated equilibrium concentrations. Given the low concentrations in the proximity of the detection limit of the GC and variations in reported thermodynamic data [41-43], the agreement between measured concentrations and calculated concentrations is good. Additionally, changes in the measured concentration closely mirror changes in the calculated equilibrium concentration over the range of conditions. A criterion that must be satisfied if *n*-butane, *n*-butene, and H_2 are at equilibrium evolves from analysis of what should be the apparent kinetics parameters for *n*-butenes, reported in Table 3. If *n*-butene concentrations are dictated by the chemical equilibrium, then the parameters will reflect thermodynamic relationships pertaining to Eq. 3, that is, the law of mass action given in Eq. 4:

$$[n\text{-}C_4H_8] = \frac{K_{DH}[n\text{-}C_4H_{10}]}{[H_2]} \quad (4)$$

With K_{DH} the equilibrium constant for Eq. 3, and brackets indicating activities of the respective species. If equilibrated, an experiment designed to determine reaction orders of *n*-butene should return values of 1 and -1 with respect to *n*-butane and H_2, and an experiment designed to determine the apparent activation energy should return 121 kJ mol^{-1}, which is the enthalpy of reaction at temperatures of 543-583 K. Indeed, the values obtained in these experiments were 1.0 to 1.2 for the reaction order with respect to *n*-butane, -0.8 to -1.0 for the reaction order with respect to H_2, and 109-130 kJ mol^{-1} for the apparent activation energy. Thus, the agreement between the parameters of the thermodynamic relationship in Eq. 3 and the experimental values is good (Table 3), which proves that *n*-butane, *n*-butenes, and H_2 are at equilibrium at the end of the catalyst bed.

Another criterion that must be satisfied if equilibrium is achieved is the independence of the *n*-butenes concentration of the space time, which was also satisfied, as shown in Figure 3. Thus, the butene gradient along a bed of Pt/H-mordenite is, under the conditions applied, minimal. The situation is different for H-mordenite; equilibrium concentration was typically not achieved with unlabeled *n*-butane (Figure 2), and when 1,4-$^{13}C_2$-*n*-butane with 120 ppm of 1-butene in the feed was used, the effluent stream still contained a quantity of *n*-butene greater than the equilibrium concentration. The rapid equilibration between butane, butenes, and H_2 on Pt/mordenite implies that the concentrations throughout the bed are known, and hence the subsequent discussion of kinetics will focus on this catalyst.

Platinum can also catalyze skeletal isomerization of butane [44] but the rate data in Table 1 give no indication of significant contributions, consistent with the low platinum loading and the high activation energy for skeletal isomerization on platinum [40].

4.3 Possible outcomes of kinetics and isotope labeling experiments

Discussion of two possible isomerization pathways, monomolecular and bimolecular, can be found in the literature. Differentiating between the two isomerization pathways requires an understanding of the experimental evidence that would prove their existence. Disproportionation products such as propane and pentane can only form through bimolecular pathways, and provide a standard for products formed through a known pathway.

The individual steps that occur in a proposed monomolecular pathway are outlined in Scheme 1. The first surface species is formed through an initiation reaction, which is almost certainly protonation of *n*-butene, because H-mordenite did not convert *n*-butane without *n*-butene in the feed (Figure 1). Hence, the concentration of active surface species is controlled by the partial pressure of *n*-butene, which presents a lower energetic barrier for protonation than *n*-butane and also has a larger heat of adsorption [45,51]. The active surface intermediate can be a π-complex, an alkoxide, or an ion pair complex. In the zeolite, an alkoxide is the most likely state in the case of short alkyl chains according to DFT calculations [46]; this picture is consistent with the observation that OH groups are consumed (as opposed to perturbed) upon adsorption of 1-pentene on H-mordenite [47]. For the cases in which platinum is present, a rate law that can be used to determine an activation energy for isomerization must consider the dehydrogenation-hydrogenation equilibrium that is preceding the isomerization, similar to the approach taken by Chiang and Bhan [48] and Macht et al. [49] for hexane isomerization. The fact that equilibrium concentrations of butenes are observed in the gas phase suggests that adsorption on the catalyst is reversible under the applied conditions and the adsorption equilibrium shown in Eq. 5, characterized by the constant K_{ads}, can be assumed:

$$n\text{-}C_4H_8(g) + S^* \leftrightharpoons n\text{-}C_4H_8 - S \quad (5)$$

With *S** a vacant surface site. Once formed, the *n*-butyl alkoxide then undergoes a monomolecular methyl shift to form an isobutyl alkoxide, which can be released into the gas phase as isobutane through either hydride transfer with *n*-butane or desorption as isobutene and hydrogenation on platinum.

If the methyl shift (Step 3 in Scheme 1) is assumed to be rate-limiting, then the rate law for monomolecular isomerization at differential conversion can be written as Eq. 6:

$$r_{mono} = \frac{k_{mono} K_1 K_2 C_T P_{n\text{-}C4H10}}{P_{H2}\left(1+\frac{K_1 K_2 P_{n\text{-}C4H10}}{P_{H2}}+\frac{P_{i\text{-}C4H10}}{K_5 K_6 P_{H2}}\right)} \quad (6)$$

Where k_{mono} is the monomolecular isomerization rate constant, K is an equilibrium constant, P is a partial pressure, and C_T is the total number of active sites. Given that the butene concentration is only a few ppm, a small fractional coverage can be assumed (implying also that the number of vacant sites [S*] is constant) and the rate law can be approximated with Eq. 7.

$$r_{mono} = k_{mono} K \frac{P_{n\text{-}C4H10}}{P_{H2}} \quad (7)$$

Thus, one would expect to measure a first order dependence on the *n*-butane partial pressure and a negative first order dependence on the H_2 partial pressure. The energy barrier in the rate constant has been investigated in DFT studies and is discussed in Section 4.4. Additionally, because there are no carbon-carbon bond breaking or bond forming events in the reaction mechanism, the number of carbon-13 isotopes in the isomerized product should be the same number as in the normal feed.

The kinetics parameters and isotope distributions for products formed through bimolecular pathways are expected to be considerably different than those for products formed through monomolecular pathways. The individual reactions in a proposed bimolecular pathway leading to formation of the disproportionation products propane and pentane are shown in Scheme 2. The C4

surface intermediates are again formed from butene, but to analyze the kinetics of disproportionation, the reaction partner of the butoxide must be identified, as both butane and butene have been suggested [13]. Alkanes without tertiary carbon atoms (i.e., *n*-butane) play only a minor role in alkylation [1] and consistently, a plot of the pentanes formation rate vs the product of butene and *n*-butane concentrations produced a series of curves. In contrast, a universal curve was obtained when plotting the pentanes formation rate vs butene concentration (see Fig. S3 in the supporting information). If beta-scission of the resulting surface C8 intermediate is the rate-limiting step, then the rate equation can be written as Eq. 8.

$$r_{bi} = \frac{k_{bi}K_1K_2K_3K_4C_T(P_{nC4H10})^2}{(P_{H2})^2\left(1+K_1K_2\left(\frac{P_{C4H10}}{P_{H2}}\right)+K_1K_2K_3\left(\frac{P_{nC4H10}}{P_{H2}}\right)^2+K_1K_2K_3K_4\left(\frac{P_{nC4H10}}{P_{H2}}\right)^2+\frac{K_1K_2}{K_7}\left(\frac{P_{iC5H12}}{P_{H2}}\right)\right)} \quad (8)$$

Where r_{bi} is the bimolecular rate and k_{bi} is the bimolecular rate constant. Under conditions at which the surface coverage is negligible, the equation simplifies to Eq. 9.

$$r_{bi} = k_{bi}K\left(\frac{P_{nC_4H_{10}}}{P_{H_2}}\right)^2 \quad (9)$$

Thus, the kinetic parameters of a product formed through a bimolecular pathway are characterized by a reaction order with respect to *n*-butene (or *n*-butane) of 2 and a reaction order with respect to H_2 of -2. The chemical reactions in the aforementioned rate equations are represented in Scheme 3 using structural formulae.

The isotope distribution in products of a bimolecular pathway will depend on the extent of isotope scrambling in C8 intermediates. Quite simply, if skeletal rearrangement of the C8 species is facile and carbon-13 isotopes are distributed randomly, then the gas phase disproportionation products will also contain a binomial distribution of isotopes. If the C8 intermediate undergoes beta-scission before a random distribution of isotopes is achieved, then the disproportionation products will not have a binomial distribution of isotopes.

4.4 Evidence for monomolecular isobutane formation at low alkene partial pressure

Both kinetics experiments and isotope labeling experiments uncovered evidence of a predominately monomolecular isomerization pathway at low alkene partial pressure. The isotope distributions in isobutane derived from isotope labeling experiments can be split into two groups: those in which isobutane contained two carbon-13 isotopes in at least 70 % of the product, and that in which only 49 % of isobutane contained two carbon-13 isotopes. The three experiments in which at least 70 % of isobutane retained two carbon-13 isotopes were characterized by a selectivity to isobutane of 77 % or greater, whereas the experiment in which only 49 % retained two carbon-13 labels delivered an isobutane selectivity of 60 %. The low amount of intermolecular isotope scrambling and high selectivity to isobutane are linked, and both are evidence of a significant contribution from a monomolecular isomerization pathway.

As discussed in section 4.3, it is possible for disproportionation products to contain a non-binomial distribution of isotopes if a random distribution of isotopes is not achieved in the C8 intermediate. In fact, Adeeva et al. [50] questioned the assumption that carbon-13 atoms in C8 intermediates are statistically scrambled during conversion of *n*-butane. When investigating the reaction pathways of 1,4-$^{13}C_2$-*n*-butane on industrial chlorided alumina catalysts, more isobutane with two carbon-13 isotopes was detected than what is expected in a binomial distribution. The authors used isobutane molecules with three and four carbon-13 atoms, which can only be formed through bimolecular pathways, as a "control" to determine if there was rapid scrambling in the C8 intermediate. Because molecules with three and four carbon-13 isotopes were not formed in a 4:1 ratio as required in a binomial distribution, the authors dismissed a monomolecular isomerization pathway as cause of the high fraction of isobutane with two carbon-13 atoms. The ratio between molecules with one and zero carbon-13 atoms, which should also be 4:1, was rejected as a criterion

because too many fragments contribute to these lower m/z values. The authors hypothesized that a concerted reaction pathway to the 2,4,4-trimethylpentenium ion exists and beta-scission occurs before carbon-13 atoms scramble. It is noteworthy that the reported internal rearrangement of carbon-13 atoms in *n*-butane of 6–25 % was lower than the conversion to gas phase products (excluding *n*-butane molecules with internally scrambled isotopes) of 10–36 % [50]. This result is consistent with a lack of intramolecular scrambling; however, it was not cited as evidence by the authors.

To assess whether the high fraction of isobutane molecules with two carbon-13 isotopes in this report was the result of a monomolecular mechanism or slow intramolecular scrambling of C8 surface species, three criteria were applied: i) the distribution of isotopomers, as considered by Adeeva et al. [50], ii) the extent of internal isotope scrambling in *n*-butane, and iii) isotope distributions in C3 and C5 side products, which can only be formed via bimolecular pathways.

Very few or no isobutane molecules with four carbon-13 isotopes were detected in the three cases in which the isotope distribution in isobutane was far from binomial (Table 2). Thus, the ratio between molecules with three and four isotopes can be taken to be greater than the ratio of four expected in a binomial distribution. However, the ratio between species with one and zero isotopes was very close to, or significantly less than, four. The most extensive scrambling was observed when a non-purified feed was used in combination with H-mordenite. In this case, the ratio between isobutane species with three and four carbon-13 isotopes was 5.9, while the ratio between species with one and zero carbon-13 isotopes was 2.6. If both ratios are considered, the criterion gives inconclusive results in all cases.

The internal isotope scrambling in *n*-butane was found to be 10–11 % for all cases (Table 4), which is much higher than the 0.5–4.5 % conversion to gas phase products. This result

demonstrates that carbon-13 isotopes are rapidly redistributed in C4 surface species and suggests (but does not prove) that rapid intramolecular scrambling is also likely in C8 species.

The isotope distribution in propane and pentanes also indicated that there was extensive isotope scrambling in C8 intermediates. For the following calculation, it was assumed that four carbon-13 isotopes were present in C8 intermediates, which disproportionate to produce propane with 0–3 isotopes and pentanes with 1–4 isotopes. The fractions of pentane molecules with zero or five carbon-13 isotopes, which deviated by up to 3 percentage points from zero, can be taken as a measure of the general uncertainty of the data and perhaps also of secondary reactions. It is obvious from Table 2 that, within this uncertainty, the isotope distributions in the pentanes are almost perfectly binomial, and the distribution is also close to binomial in propane. Analysis of the isotope distributions in the side products demonstrates that intramolecular scrambling in C8 intermediates is fast, and a non-binomial isotope distribution in isobutane cannot be the result of a bimolecular pathway with limited isotope redistribution in C8 intermediates. It follows that a small portion of the isobutane was produced via a monomolecular pathway on H-mordenite when an unpurified feed was used, and significant portions of isobutane were produced by a monomolecular pathway in experiments with the three other feed–catalyst combinations.

With the evidence from isotope labeling experiments that a substantial portion of isobutane is produced via a monomolecular pathway when the concentration of butene is sufficiently low, one can evaluate the kinetics data collected from conversion of unlabeled *n*-butane on Pt/H-mordenite. It should first be noted that mass transport was eliminated as being the source of rate control using calculations described in Sections S4 and S5 of the Supporting Information. In the kinetics experiments on Pt/H-mordenite, equilibration between *n*-butane, *n*-butene, and H_2 was rapid, and the gas phase concentration of butene was thus known along the length of the catalyst

bed. The reaction order for isobutane with respect to *n*-butane or *n*-butene was 1.0 to 1.2 over the range of conditions, as illustrated in Figure 4 and reported in detail in Table S7 of the supporting information. The reaction order with respect to H_2 was -0.8 to -1.1. Both reaction orders are those expected in the case of a predominately monomolecular mechanism, whereas the slight increase in reaction order with respect to *n*-butane with decreasing partial pressure indicates increasing participation of the bimolecular pathway. One must keep the butene partial pressure in mind when reading Figure 4; because of the facile equilibration of alkane, alkene, and H_2, the butene partial pressure increases as the H_2 partial pressure is lowered, and one would thus expect increasing contributions from bimolecular pathways that are second order with respect to butene.

To compare these results with published reaction orders with respect to *n*-butane, one must make assumptions regarding butene concentrations in the reported experiments because they are generally not reported. In the absence of platinum (or any other suitable metal), equilibration according to Eq. 3 relies on the intrinsic activity of the zeolite and is not likely. Measured activation energies for dehydrogenation on an H-form zeolite range from 189 to 204 kJ mol^{-1} [38]. If platinum is present, equilibration is attained and Eq. 3 is valid. If H_2 is co-fed in ratios as those used here then the formed H_2 will change the overall H_2 concentration only marginally and the butenes equilibrium concentration will be proportional to the *n*-butane concentration. If *n*-butane is fed without H_2, then the equilibrium concentration of *n*-butene is proportional to the square root of the *n*-butane concentration (and an order of 1 with respect to *n*-butane can be consistent with a bimolecular mechanism).

The following literature data are for platinum-free mordenite, making it difficult to judge what the butene concentration in the reactor might have been. Apparent orders for isobutane formation with respect to *n*-butane of 1 (with H_2 added) [21] and 0–1.25, 1.17, or 2 (no H_2 added) [13,21,23]

have been reported. Apparent orders for pentanes formation of 2 with respect to isobutane (with H_2 added) [8] or 1.9 with respect to *n*-butane (no H_2 added) [23] have been observed. This report clarifies that the reaction order of 1 for isobutane is in fact linked to a monomolecular pathway and is not the result of a pseudo-first order bimolecular pathway. It also clarifies that isobutane can be produced through both monomolecular (first order with respect to *n*-butene) and bimolecular (second order with respect to *n*-butene) pathways, and it is thus conceivable that the choice of reaction parameters determines the apparent order that is measured.

With the knowledge that isomerization rates are first order with respect to *n*-butene, an apparent first order rate constant can be calculated if the change in butene concentration with temperature (as the equilibrium shifts with temperature) is considered. The calculated concentrations of *n*-butene were used to avoid the uncertainty inherent to the measured values. Arrhenius plots using the apparent first order rate constants (the product of k_{isom} and K_{ads}) were constructed for a number of conditions, whereby the R^2 values were 0.993 or greater and the uncertainty was ± 8 kJ mol^{-1}. An example Arrhenius plot is shown in Fig. S4 in the supporting information. The resulting apparent activation energy for isobutane formation was 20-24 kJ mol^{-1}. The apparent activation energy is related to the true activation energy by the enthalpy of adsorption according to Eq. 10:

$$E_a = E_{app} - \Delta H_{ads} \quad (10)$$

Where E_a is the true activation energy, E_{app} is the apparent activation energy, and ΔH_{ads} is the enthalpy of adsorption. Thus, if the enthalpy of adsorption can be determined, then the true activation energy can be calculated.

Fogash et al. [27] estimated the enthalpy of adsorption for butene on H-mordenite to be −100 kJ mol^{-1} using a correlation between the enthalpy of adsorption and the gas phase proton

affinity. Lechert and Schweitzer [51] reported an experimentally determined enthalpy of adsorption of 110 kJ mol^{-1} for 1-butene on H-MFI at a temperature of 523 K. Gomes et al. [52] recently corroborated the value with DFT calculations. Combining these enthalpies of adsorption from the literature with the experimentally determined apparent activation energy of 20–24 kJ mol^{-1} yields a true activation energy of 120-134 kJ mol^{-1}.

True activation energies have been obtained by DFT, which can deliver energies for elementary steps such as the rearrangement of the adsorbed butyl. Boronat et al. [53] found the activation energy of the skeletal rearrangement step of *n*-butene on a Theta-1 cluster to be 110 to 145 kJ mol^{-1} depending on the basis set that was used. More recently, Wattanakit et al. [54] found the activation energy of the same step to be 87 kJ mol^{-1} on H-ferrierite. Gleeson [55] predicted the activation energy of carbenium ion and alkoxide based mechanisms to be 103 and 143 kJ mol^{-1}, respectively, on H-ferrierite. The framework type generally affects the enthalpy of alkane adsorption and the apparent activation energy of isomerization, but not the true activation energy [56]. Hence, the reported computational results and the experimentally determined value for the true activation energy for butyl rearrangement agree within their respective error margins. Skeletal rearrangement of the adsorbed C4 species must be the rate-determining step, followed by facile hydride transfer from an incoming reactant molecule to liberate the product and close the catalytic cycle.

Previously reported apparent activation energies for isobutane formation on Pt/H-mordenite were between 44 and 71 kJ mol^{-1} and found to depend on the hydrogen to hydrocarbon ratio [24]. Because fits of deactivation and extrapolation to time equals zero were used to generate the values, the authors stated that they were “to be taken with care in mechanistic considerations”. To date, these values are the only activation energies reported for butane isomerization on a zeolite.

Domokos et al. [57] measured the apparent activation energy of isobutene and isobutane formation from *n*-butene on H-ferrierite and found them to be 59 and 28 kJ mol^{-1}, respectively. The authors hypothesized that desorption is the rate-limiting step for isobutene formation, but did not comment on the rate-limiting step for isobutane. The reported apparent activation energy for isobutane is close to the value of 20–24 kJ mol^{-1} reported in this manuscript.

The combined evidence from kinetics and isotope experiments suggests that a monomolecular isomerization pathway is the dominant isomerization pathway under conditions at which the partial pressure of alkene is sufficiently low. But, if the claim is correct, then questions remain about the alleged formation of a primary carbenium ion along the reaction coordinate. If one accepts that isomerization is preceded by dehydrogenation, then the DFT calculations performed by Boronat et al. [58] concerning the skeletal isomerization of linear butenes on a zeolite are pertinent. (In principle, the two reaction sequences should differ only in the initiation and termination steps; the rearrangement steps should be identical.) The authors determined that the transition state for monomolecular skeletal isomerization of butene comprises a cyclopropane ring that maintains elongated C-O bonds with the zeolite lattice and thus does not resemble a primary carbenium ion. Upon opening of the cyclopropane ring, a primary alkoxide is formed, which is lower in enthalpy than the cyclopropane ring, and is a minimum on the potential energy surface. The transition state in the skeletal isomerization pathway catalyzed by liquid superacids is distinctly different; in this case, the transition state is the species formed upon opening of the cyclopropane ring, which must result in formation of a primary carbenium ion [17]. This difference between solid and liquid acids can be understood when comparing the properties of the respective anions: the nucleophilicity of oxygen anions in the zeolite framework is suited for the formation of an alkoxide, whereas the

anions in superacids lack any nucleophilicity, thus making possible the existence of free carbenium ions.

4.5 Evidence that bimolecular pathways dominate at "high" alkene partial pressure

Although there is clear evidence that isobutane formation is in large part monomolecular under conditions of low alkene partial pressure, the significant amount of intermolecular isotope scrambling when butene was co-fed suggests that there are also bimolecular isomerization pathways that are favored by high alkene partial pressure. Thus, a discussion of the bimolecular pathway and formation of disproportionation products is prudent.

The data for propane and pentanes (Table 5) are largely consistent with what one expects for a bimolecular dimerization-cracking pathway. The isotope distributions for both products, when they were produced in concentrations high enough to measure complete mass spectra, were binomial within error. The result is in good agreement with Guisnet et al. [20], who converted 1-^{13}C-*n*-butane on H-mordenite and found a binomial distribution of carbon-13 in pentanes over a wide range of conversions.

The pentane reaction order with respect to *n*-butene was 1.4–2.2, with deviations from 2 at high temperatures and low H_2 partial pressures, that is, at higher butene concentrations. The obtained fractional order of less than 2 could be an indication of increasing surface coverage, which would invalidate the omission of the denominator in a rate law derived using a Langmuir adsorption model. If that is the case, then the reaction order for isobutane formation with respect to butenes would also be affected by coverage and the participation of a bimolecular mechanism could be somewhat higher than suggested. Overall, the higher-than-1 order with respect to *n*-butene for pentanes formation is consistent with a bimolecular pathway, but the changing orders between 1.4 and 2.2 are not fully understood.

If beta-scission of the isomerized C8 surface species (Step 5 of Scheme 2) is assumed to be the rate-limiting step, the apparent activation energy can be extracted using the same method as for isobutane. The energies for pentane covered a wider range than those for isobutane, but were generally around -20 kJ mol^{-1}. Using an enthalpy of adsorption of a C8 alkene of -160 kJ mol^{-1}, calculated using the method of Fogash et al. [27], a true activation energy around 140 kJ mol^{-1} is calculated. This value is in reasonable agreement with a reported value of 153 kJ mol^{-1} obtained computationally by Mazar et al. [59] for beta-scission of 3,3-dimethylhexoxide on H-ZSM-5.

Since the skeletal rearrangement of C8 species is facile, as indicated by the binomial distribution of isotopes in disproportionation products, a distribution of skeletal isomers that closely resembles the distribution expected at chemical equilibrium can be assumed. In the gas phase at a temperature of 600 K, the equilibrium composition of C8 isomers with 0, 1, 2, and 3 methyl branches is 10, 43, 37, and 3.4 mol %, respectively [60]. De Lucas et al. [61] converted *n*-octane on Pt/H-mordenite at 603 K and already at 50 % conversion found the isomer distribution to consist entirely of species with only one or two methyl branches, which is largely consistent with the gas phase equilibrium composition. The absence of species with three methyl branches suggests that there is not a transition state selectivity favoring formation of these species. An argument had been put forth that 2,2,4-trimethylpentane is selectively formed from *n*-butane and cracks to eventually make two isobutane molecules [62]. In light of the findings of de Lucas et al [61] and an equilibrium content of 2,2,4-trimethylpentane at 600 K of only 1.5 mol % [60], this preferential pathway is not a likely scenario.

The extent of branching in the surface C8 species greatly impacts the cracking products, as shown in the inclusive list of pathways in Scheme S1 in the supporting information. It is true that 2,2,4-trimethylpentane produces isobutane with high selectivity; Lugstein et al. [63] hydrocracked

the species on Ni/H-mordenite and found an isobutane to (propane + pentanes) ratio of 21. A ratio of only 1.4 was found when 2,5-dimethylhexane was hydrocracked [63]. *n*-Octane has been hydrocracked on various mordenites and ratios of 1.1 [61,63] and 0.5 [64] have been found. Simonetti et al. [65] converted triptene in the presence of dimethyl ether on H-beta and found a high selectivity to isobutyl product, presumably through methylation and subsequent cracking. Thus, when the zeolite is presented with a triply-methylated C8 species, the species does crack to selectively product isobutane. However, given that triply-methylated C8 species are not the primary products of *n*-butene dimerization, and are not thermodynamically favored (i.e., there is no driving force for the subsequent isomerization reactions to form them), a dimerization-cracking pathway starting from *n*-butane that produces isobutane with high selectivity seems unlikely.

With the understanding that dimerization–cracking reactions are not likely to produce isobutane with high selectivity, and the additional evidence that a monomolecular isomerization pathway contributes significantly to isobutane formation, we are in a position to explain variations in selectivity with varying reaction conditions. Such variations were previously noted in the literature [6,13,24] but lacked a consistent interpretation. Asuquo et al. [13] observed that the selectivity to isobutane was higher at low temperatures, but claimed that the activation energy of a monomolecular pathway was too high for it to contribute significantly to the product contribution. Tran et al. [6] diluted *n*-butane in either H_2 or N_2 and associated variations in selectivity with the concentration of *sec*-butyl carbenium ions. Specifically, they proposed that the bimolecular pathway requires two carbenium ions and consequently should be more sensitive to a decrease in the concentration of carbenium ions caused by the presence of hydrogen.

The data shown in Figure 3 clarifies that butene concentration is the variable that controls selectivity to isobutane or disproportionation products. The data was collected on Pt/H-mordenite,

so under all conditions the butene concentration was controlled by chemical equilibrium with butane and H_2. Thus, one must read Figure 3 while considering how the butene concentration changes with reaction conditions. A change in any reaction condition that caused the butene concentration to increase (i.e. raising the temperature, raising the *n*-butane partial pressure, or lowering the H_2 partial pressure) caused a dramatic drop in selectivity to isobutane and a dramatic increase in selectivity to pentanes. The only reaction parameter that caused an increase in conversion but did not affect the butene concentration is the space time; when the space time was increased, the drop in selectivity to isobutane was only 3 %. The changes in selectivity with changing butene concentration are explained by their different reaction orders with respect to *n*-butene.

4.6 Reconciliation of observations with previous results from conversion of carbon-13 labeled butane

The data presented in this contribution implicates the butene concentration as the variable that most strongly impacts the skeletal isomerization pathways of *n*-butane (either mono- or bimolecular). Consequently, the butene concentration also affects the extent of isotope scrambling in isobutane. Isotope scrambling in isobutane increased with increasing butene concentration, whereas the isotope distribution in propane and pentane was independent of the butene concentration. With this knowledge, contradictory reports in the literature can be reconciled and a unified model can be formulated. A summary of previous investigations in which labeled butanes were used to elucidate their skeletal isomerization mechanism on solid acids is given in Table 6.

The first investigation using carbon-13 labeled butane on H-mordenite was performed by Bearez et al. [10], and to our knowledge is the only paper reporting full isotope distributions in all products. Another paper reports only selected results [9]. Using a recirculation reactor with

1-^{13}C-isobutane as the reactant, the isotope distribution in propane, *n*-butane, and isopentane products was measured as a function of conversion. Because isotope scrambling was detected in the three main products, a disproportionation mechanism involving formation of a C8 carbenium ion as the rate-limiting step was proposed. However, the data clearly show that the isotope composition of propane and isopentane did not change over the range of conversion investigated (≈ 15–50 %), while the isotope composition of the skeletal isomerization product, *n*-butane, changed significantly with conversion. Less isotope scrambling was observed at 15 % conversion compared to the binomial distribution that was reached at 40 % conversion. In fact, the isotope distribution in *n*-butane mirrored that of the isobutane reactant, not that of the propane and isopentane disproportionation products. The non-changing binomial isotope distribution in propane and isopentane demonstrates that isotopes in C8 intermediates were statistically scrambled. Thus, if *n*-butane was formed through similar bimolecular pathways as the disproportionation products, the isotope distribution should also be binomial over the entire range of conversion. An alternative explanation of that data is that the main pathway of *n*-butane formation at low conversion was probably monomolecular. At higher conversions, when secondary reactions are more likely, *n*-butane formed as a monomolecular product entered bimolecular reaction cycles that caused isotope scrambling, and the isotopic evidence of a monomolecular pathway was slowly erased.

Sachtler and co-workers used 1,4-$^{13}C_2$-*n*-butane, like the one in this work from Isotec Inc. (impurities not reported), in a recirculation reactor on a variety of industrial chlorided alumina catalysts [66] and platinum-free sulfated zirconia catalysts [67-69]. In all cases, a conclusion was reached that the operating mechanism of isobutane formation was predominately bimolecular. When any form of sulfated zirconia was used, the isotope distribution was reported at 40-60 %

conversion. In these experiments, the high conversion may have erased any evidence that existed at lower conversions for a monomolecular pathway. In fact, the authors stated that the isobutane product contained exclusively two carbon-13 atoms at low conversion. In the previously discussed report of Bearez et al. [10], the distribution of carbon-13 isotopes became almost completely binomial at about 40 % conversion. Another possible way to interpret Sachtler's data is that alkene impurities, if present in the feed, promoted isotope scrambling as seen in the data reported in this paper. In contrast to the reports of Sachtler, Garin et al. [70] found far less intermolecular isotope scrambling on sulfated zirconia and Pt/sulfated zirconia. In this case, conversions were only 8–18 %, and a carefully purified homemade feed was used. The carefully purified feed and perhaps also the added H_2 excluded significant alkene concentrations in the reactor, and the low conversion limited secondary reactions, thus allowing for isotopic evidence of a monomolecular pathway to be collected.

Finally, the skeletal isomerization mechanism on sulfated zirconia, WO_3/ZrO_2, and the heteropoly compound $Cs_{2.5}H_{0.5}PW_{12}O_{40}$ was found to depend on the presence of platinum and H_2 by Okuhara and co-workers [71,72]. Platinum and H_2, for unknown reasons, promoted the monomolecular pathway, as determined by the isotope distributions in gas phase products. The 1,4-$^{13}C_2$-*n*-butane in these experiments was also from Isotec, Inc. (with the impurities not reported), conversions were around 10 %, and H_2 was used only in combination with catalysts containing platinum. The results mirror those presented in this paper; extensive isotope scrambling was seen on catalysts lacking platinum, and far less scrambling was seen on platinum-containing catalysts with H_2 in the feed, thus under conditions implying low butene concentrations. As demonstrated in this work, the operating mechanism is not *directly* impacted by the platinum on

the catalyst or H_2 in the feed, but instead is *indirectly* impacted by their ability to control the gas phase concentration of alkenes.

5 Conclusion

Reaction pathways of *n*-butane on H-mordenite are shown to depend on the concentration of *n*-butenes in the catalyst bed. In the presence of platinum on the catalyst, *n*-butenes are found in equilibrium concentrations with *n*-butane and H_2. Isobutane formation has a first order dependence on the *n*-butene concentration over a wide range of conditions, suggesting isomerization by a monomolecular mechanism. The apparent activation energy for isobutane formation, considering a first order reaction in butene, is 20–24 kJ mol^{-1}. The calculated true activation energy of 120–134 kJ mol^{-1} is in agreement with activation energies previously obtained by DFT for *n*-butene isomerization, supporting the hypothesis of a monomolecular mechanism. With minimized butene levels in the reactor, as much as 81% of the isobutane product from 1,4-$^{13}C_2$-*n*-butane contained 2 carbon-13 isotopes, consistent with predominantly monomolecular isomerization. In contrast, with only 120 ppm of 1-butene in the feed and a catalyst with poor hydrogenation capability (H-mordenite without platinum), the majority of the isobutane product molecules contained a number of carbon-13 isotopes not equal to two.

Bimolecular reaction pathways produce both disproportionation products and isomerization product. Disproportionation products have a higher order dependence on butene, and, reaction conditions that result in “high” butene concentrations favor bimolecular pathways that are non-selective to the desired product, isobutane. Contributions of a bimolecular mechanism to isobutane formation at higher butene concentrations are evident through an increase in reaction order.

The observation that product formation rates, selectivities, and isotope distributions all depend on the partial pressure of butene forms a convincing argument that a relevant monomolecular skeletal isomerization pathway exists for *n*-butane on H-mordenite and Pt/H-mordenite. Previous discrepancies in the literature relating to isotope distributions in products obtained from carbon-13 labeled butane can be rationalized as the result of varying alkene concentrations (produced in the reactor or present as impurity in the feed). Furthermore, it appears that one of the main roles of platinum and H_2, which are ingredients in commercial processes, is to control the gas phase and thus the surface alkene concentration.

6 Acknowledgements

This work was, in part, supported by the NSF EPSCoR award EPS 0814361 and NSF Award 0923247. The authors thank UOP LLC, a Honeywell company, for kindly providing the zeolite samples. M.J.W. thanks the Graduate Student Senate at the University of Oklahoma for a research grant.

References

[1] A. Feller, J.A. Lercher, Adv. Catal. 48 (2004) 229.
[2] S. van Donk, J.H. Bitter, K.P. de Jong, Appl. Catal., A 212 (2001) 97.
[3] H. Pines, R.C. Wackher, J. Am. Chem. Soc. 68 (1946) 595.
[4] D.M. Brouwer, Recl. Trav. Chim. Pay.-B. 87 (1968) 1435.
[5] N.N. Krupina, A.L. Proskurnin, A.Z. Dorogochinskii, React. Kinet. Catal. Lett. 32 (1986) 135.
[6] M.T. Tran, N.S. Gnep, G. Szabo, M. Guisnet, J. Catal. 174 (1998) 185.
[7] Y. Ono, Catal. Today 81 (2003) 3.
[8] C. Bearez, F. Chevalier, M. Guisnet, React. Kinet. Catal. Lett. 22 (1983) 405.
[9] M. Guisnet, N.S. Gnep, Appl. Catal. A 146 (1996) 33.
[10] C. Bearez, F. Avendano, F. Chevalier, M. Guisnet, B. Soc. Chim. Fr. 3 (1985) 346.
[11] M.T. Tran, N.S. Gnep, G. Szabo, M. Guisnet, Appl. Catal. A 170 (1998) 49.
[12] R.A. Asuquo, G. Eder-Mirth, K. Seshan, J.A.Z. Pieterse, J.A. Lercher, J. Catal. 168 (1997) 292.
[13] R.A. Asuquo, G. Eder-Mirth, J.A. Lercher, J. Catal. 155 (1995) 376.
[14] D.M. Brouwer, H. Hogeveen, in A. Streitwieser, Jr., R.W. Taft (Eds.), Progress in Physical Organic Chemistry, vol. 9,Wiley-Interscience, New York, 1972, p. 179.
[15] D.M. Brouwer, J.M. Oelderik, Recl. Trav. Chim. Pay.-B. 87 (1968) 721.
[16] Y. Ono, Catal. Today 81 (2003) 3.
[17] M. Boronat, P. Viruela, A. Corma, J. Phys. Chem. 100 (1996) 633.
[18] M.T. Tran, N.S. Gnep, G. Szabo, M. Guisnet, Appl. Catal., A 170 (1998) 49.
[19] M. Guisnet, N.S. Gnep, Appl. Catal., A 146 (1996) 33.
[20] C. Bearez, F. Avendano, F. Chevalier, M. Guisnet, B. Soc. Chim. Fr. 3 (1985) 346.
[21] M.T. Tran, N.S. Gnep, G. Szabo, M. Guisnet, J. Catal. 174 (1998) 185.
[22] N.N. Krupina, A.L. Proskurnin, A.Z. Dorogochinskii 32 (1986) 135.
[23] P. Cañizares, A. de Lucas, F. Dorado, Appl. Catal., A 196 (2000) 225.
[24] V. Nieminen, M. Kangas, T. Salmi, D.Y. Murzin, Ind. Eng. Chem. Res. 44 (2005) 471.
[25] H. Pines, R.C. Wackher, J. Am. Chem. Soc. 68 (1946) 595.
[26] K.B. Fogash, Z. Hong, J.M. Kobe, J.A. Dumesic, Appl. Catal., A 172 (1998) 107.
[27] K.B. Fogash, Z. Hong, J.A. Dumesic, J. Catal. 173 (1998) 519.
[28] J. Engelhardt, J. Catal. 164 (1996) 449.
[29] H. Liu, V. Adeeva, G.D. Lei, W.M.H. Sachtler, J. Mol. Catal. A: Chem. 100 (1995) 35.
[30] J.E. Tabora, R.J. Davis, J. Am. Chem. Soc. 118 (1996) 12240.
[31] N. Lohitharn, J.G. Goodwin, E. Lotero, J. Catal. 234 (2005) 199.
[32] N. Lohitharn, E. Lotero, J.G. Goodwin, J. Catal. 241 (2006) 328.
[33] N. Lohitharn, J.G. Goodwin, J. Catal. 245 (2007) 198.
[34] T. Suzuki, T. Okuhara, Catal. Lett. 72 (2001) 111.
[35] T. Echizen, T. Suzuki, Y. Kamiya, T. Okuhara, J. Mol. Catal. A: Chem. 209 (2004) 145.
[36] P.B. Weisz, E.W. Swegler, Science 126 (1957) 31.
[37] M. Chiappero, P.T.M. Do, S. Crossley, L.L. Lobban, D.E. Resasco, Fuel 90 (2011) 1155.
[38] R. Gounder, E. Iglesia, J. Catal. 277 (2011) 36.
[39] M.J. Wulfers, F.C. Jentoft, J. Catal. 307 (2013) 204.
[40] D.E. Resasco, in I.T. Horvath (Ed.), Encyclopedia of Catalysis, vol. 3, John Wiley & Sons, Hoboken, NJ, 2002.

[41] M.D. Koretsky, Engineering and Chemical Thermodynamics, Wiley, Hoboken, NJ, 2004.
[42] E.J. Prosen, F.W. Maron, F.D. Rossini, J. Res. NBS, 46 (1951) 106.
[43] C.L. Yaws, Yaws' Handbook of Thermodynamic and Physical Properties of Chemical Compounds, Norwich, NY, 2003.
[44] F. Rodriguez-Reinoso, I. Rodrigues-Ramos, C. Moreno-Castilla, A. Guerrero-Ruiz, J.D. Lopez-Gonzalez, J. Catal. 107 (1987) 1.
[45] J.A. van Bokhoven, M. Tromp, D.C. Koningsberger, J.T. Miller, J.A.Z. Pieterse, J.A. Lercher, B.A. Williams, H.H. Hung, J. Catal. 202 (2001) 129.
[46] H. Fang, A. Zheng, J. Xu, S. Li, Y. Chu, L. Chen, F. Deng, J. Phys. Chem. C 115 (2011) 7429.
[47] M.J. Wulfers, F.C. Jentoft, J. Catal. 307 (2013) 204.
[48] H. Chiang, A. Bhan, J. Catal. 283 (2011) 98.
[49] J. Macht, R.T. Carr, E. Iglesia, J. Am. Chem. Soc. 131 (2009) 6554.
[50] V. Adeeva, W.M.H. Sachtler, Appl. Catal. A 163 (1997) 237.
[51] H. Lechert, W. Schweitzer, in Proceedings of the 6th International Zeolite Conference, D. Olson, A. Bisio Eds., Butterworths, Washington D.C., 1983, p. 210.
[52] J. Gomes, P.M. Zimmerman, M. Head-Gordon, A.T. Bell, J. Phys. Chem. C 116 (2012) 15406.
[53] M. Boronat, P. Viruela, A. Corma, Phys. Chem. Chem. Phys. 3 (2001) 3235.
[54] C. Wattanakit, S. Nokbin, B. Boekfa, P. Pantu, J. Limtrakul, J. Phys. Chem. C 116 (2012) 5654.
[55] D. Gleeson, J. Phys. Chem. A 115 (2011) 14629.
[56] A. van de Runstraat, J.A. Kamp, P.J. Stobbelaar, J. van Grondelle, S. Krijnen, and R.A. van Santen, J. Catal. 171 (1997) 77–84.
[57] L. Domokos, L. Lefferts, K. Seshan, J.A. Lercher, J. Catal. 197 (2001) 68.
[58] M. Boronat, P. Viruela, A. Corma, J. Phys. Chem. A 102 (1998) 982.
[59] M.N. Mazar, S. Al-Hashimi, M. Cococcioni, A. Bhan, J. Phys. Chem. C 117 (2013) 23609.
[60] R. A. Alberty, E. Burmenko, J. Phys. Chem. Ref. Data 13 (1986) 1173.
[61] A. de Lucas, J.L Valverde, P. Sanchez, F. Dorado, M.J. Ramos, Appl. Catal., A 282 (2005) 15.
[62] V. Adeeva, W.M.H. Sachtler, Appl. Catal., A 163 (1997) 237.
[63] A. Lugstein, A. Jentys, H. Vinek, Appl. Catal., A 176 (1999) 119.
[64] J.M. Grau, J.M. Parera, Appl. Catal., A 162 (1997) 17.
[65] D.A. Simonetti, J.H. Ahn, E. Iglesia, J. Catal. 277 (2011) 173.
[66] V. Adeeva, W.M.H. Sachtler, Appl. Catal. A 163 (1997) 237.
[67] H. Liu, V. Adeeva, G.D. Lei, W.M.H. Sachtler, J. Mol. Catal. A: Chem. 100 (1995) 35.
[68] V. Adeeva, G.D. Lei, W.M.H. Sachtler, Catal. Lett. 33 (1995) 135.
[69] V. Adeeva, G.D. Lei, W.M.H. Sachtler, Appl. Catal. A 118 (1994) L11.
[70] F. Garin, L. Seyfried, P. Girard, G. Maire, A. Abdulsamad, J. Sommer, J. Catal. 151 (1995) 26.
[71] T. Echizen, T. Suzuki, Y. Kamiya, T. Okuhara, J. Mol. Catal. A: Chem. 209 (2004) 145.
[72] T. Suzuki, T. Okuhara, Catal. Lett. 72 (2001) 111.

Figures

Figure 1

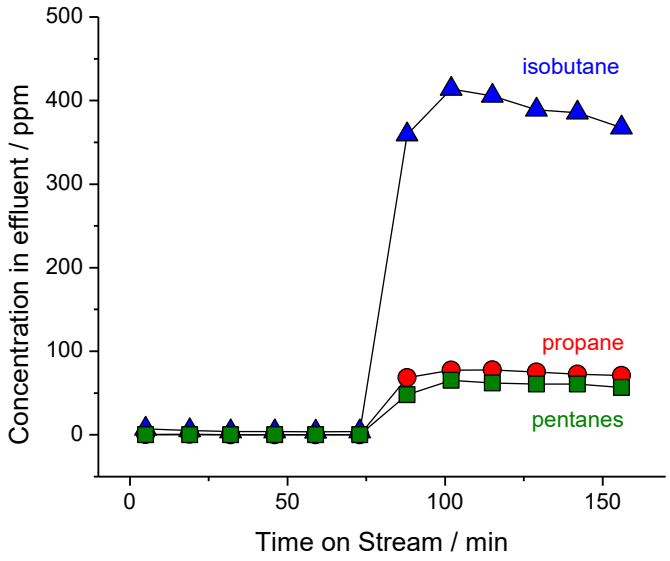

Figure 1: The concentration of gas phase products resulting from conversion of *n*-butane (10 kPa partial pressure) on H-mordenite at a temperature of 473 K using 50 kPa H_2 and 40 kPa helium as diluents. The concentration of *n*-butenes in the feed was 0 ppm during the first 75 min on stream and 18 ppm after 75 min on stream.

Figure 2

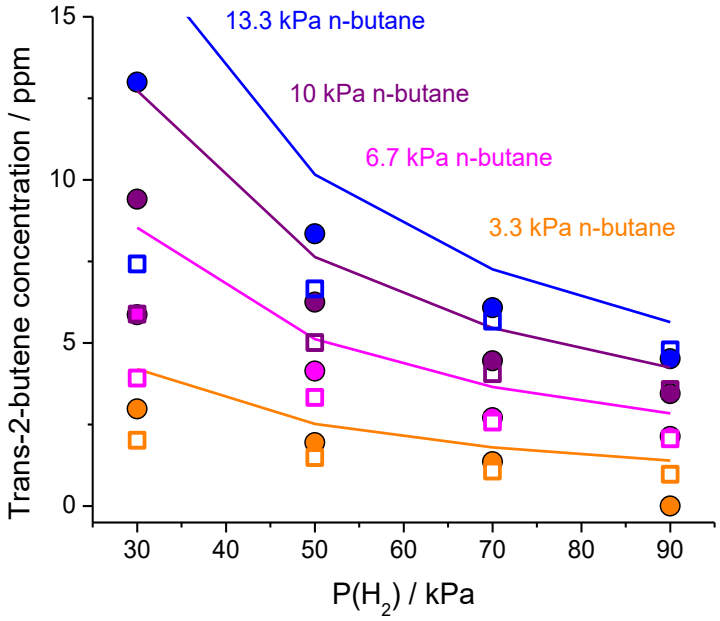

Figure 2: Measured concentrations and calculated equilibrium concentrations of *trans*-2-butene at a temperature of 563 K over the range of *n*-butane and H_2 partial pressures. Solid circles: measured on Pt/H-mordenite. Open squares: measured on H-mordenite. Lines: calculated equilibrium concentrations using the software package Thermosolver (v. 1.0).

Figure 3

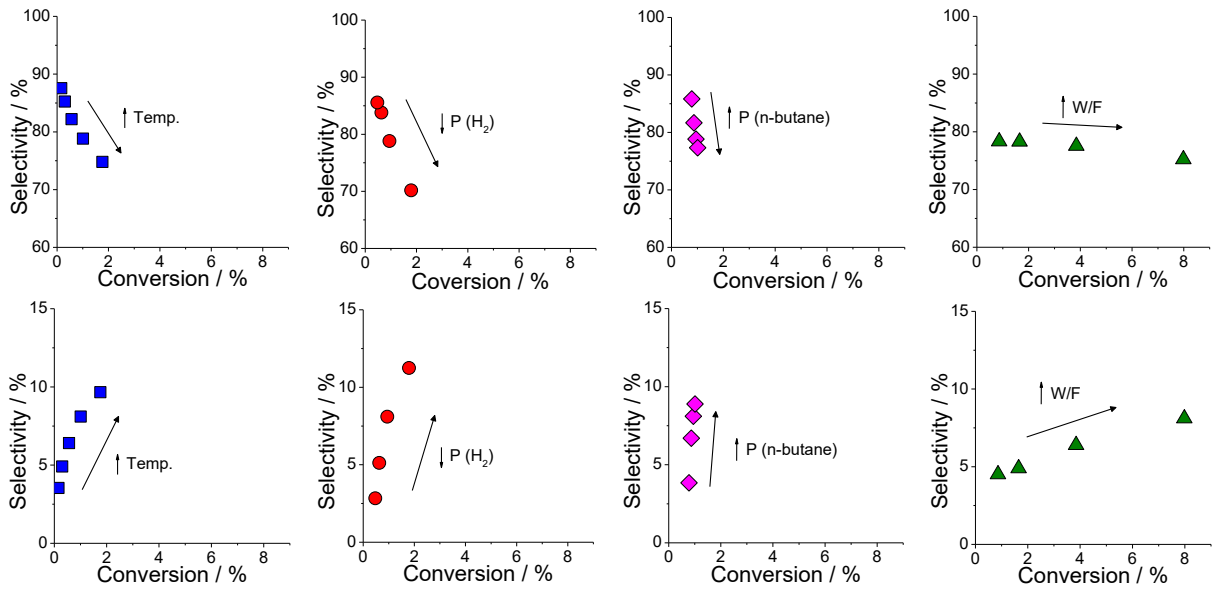

Figure 3: Selectivities of isobutane (upper row) or pentanes (lower row) on Pt/H-mordenite with respect to conversion. Changes in conversion were caused by changes in temperature (blue squares: 543-583 K, 10 kPa *n*-butane, 50 kPa H_2, W/F = 0.17 h), H_2 partial pressure (red circles: 573 K, 10 kPa *n*-butane, 30-90 kPa H_2, W/F = 0.17 h), *n*-butane partial pressure (magenta diamonds: 573 K, 3.3-13.3 kPa *n*-butane, 50 kPa H_2, W/F = 0.13-0.51 h), or space time (green triangles: 573 K, 10 kPa *n*-butane, 50 kPa H_2, W/F = 0.13-1.29 h).

Figure 4

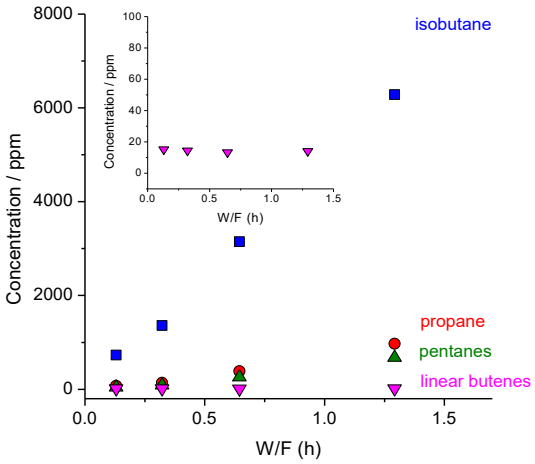

Figure 4: Concentration of the main gas phase products produced from conversion of *n*-butane on Pt/H-mordenite. Conditions: reaction temperature 573 K, 50 ml min^{-1} total flow, 50 kPa H_2, 40 kPa helium, W/F = 0.13-1.29 h.

Figure 5

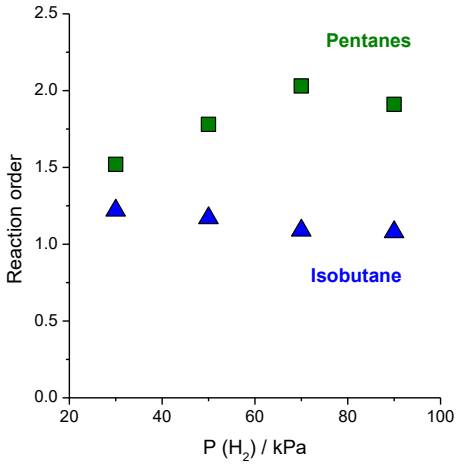

Figure 5: Reaction orders with respect to *n*-butene for isobutane and pentanes on Pt/H-mordenite at a temperature of 573 K, *n*-butane partial pressure of 10 kPa, and H_2 partial pressures between 30 and 90 kPa.

Table 1: Rates and selectivities of major products produced from 1,4-$^{13}C_2$-*n*-butane or unlabeled *n*-butane at a temperature of 573 K and *n*-butane partial pressure of 10 kPa.

	$P(H_2)$ / kPa	Purified feed	Rate / μmolg^{-1}h^{-1}			Selectivity / mol %			*n*-Butene concentration / ppm	
			Isobutane	Propane	Pentanes	Isobutane	Propane	Pentanes	Measured	Equilib.
Labeled feed										
H-mordenite	70	No	1770	755	330	60	25	11	32	16
Pt/H-mordenite[a]	90	No	370	62	37	77	13	8	12	13
H-mordenite	70	Yes	765	110	75	78	11	8	17	16
Pt/H-mordenite	70	Yes	495	46	30	83	8	5	12	16
Unlabeled feed										
H-mordenite	70	n/a	555	55	43	81	8	6	12	16
H-mordenite	90	n/a	498	45	33	82	7	5	10	13
Pt/H-mordenite	70	n/a	537	40	33	84	6	5	14	16
Pt/H-mordenite	90	n/a	422	24	14	86	5	3	11	13

[a] measured with GC-MS

Table 2: Isotope distributions in products produced from 1,4-$^{13}C_2$-*n*-butane

		Number of ^{13}C isotopes / %					
Catalyst	**Trap**	**0**	**1**	**2**	**3**	**4**	**5**
Isobutane							
H-mordenite	No	8	19	49	21	4	
Pt/H-mordenite	No	3	14	72	10	0	
H-mordenite	Yes	7	9	70	13	1	
Pt/H-mordenite	Yes	9	3	81	7	0	
Binomial		*6.2*	*25*	*37.5*	*25*	*6.2*	
Propane							
H-mordenite	No	10	41	39	10		
H-mordenite	Yes	9	45	38	7		
Binomial		*12.5*	*37.5*	*37.5*	*12.5*		
2-Methylbutane							
H-mordenite	No	2	14	36	34	13	2
H-mordenite	Yes	1	10	39	39	10	0
*Binomial**		*0*	*12.5*	*37.5*	*37.5*	*12.5*	*0*
***n*-Pentane**							
H-mordenite	No	1	14	36	35	13	2
H-mordenite	Yes	-3	9	40	43	11	0
*Binomial**		*0*	*12.5*	*37.5*	*37.5*	*12.5*	*0*

*considering that C8 intermediates contain a maximum of four carbon-13 isotopes

Table 3: Comparison of experimentally determined apparent kinetic parameters and parameters expected at equilibrium for *n*-butenes on Pt/H-mordenite

Parameter	Experimental Value	Equilibrium Value
n-Butane reaction order	1.0 to 1.2	1.0
H_2 reaction order	-1.0 to -0.8	-1.0
Apparent activation energy / kJ mol^{-1}	109 – 130 kJ mol^{-1}	121 kJ mol^{-1}

Table 4: Percent of 1,4-$^{13}C_2$-*n*-butane with internally scrambled carbon-13 atoms after conversion on H-mordenite or Pt/H-mordenite.

Catalyst	Trap	Internal scrambling / %
H-mordenite	No	11.0
H-mordenite	Yes	10.1
Pt/H-mordenite	No	9.7
Pt/H-mordenite	Yes	10.9

Table 5: Apparent kinetics parameters on Pt/H-mordenite

Parameter	Isobutane	Pentanes
Reaction order with respect to *n*-butene	0.9 to 1.2	1.4 to 2.2
Reaction order with respect to H_2	-0.8 to -1.1	-2.1 to -2.7
Apparent activation energy / kJ mol^{-1}	20 to 24 kJ mol^{-1}	~ -20 kJ mol^{-1}

Table 6: Summary of reaction conditions employed in previous reports in which isotopically labeled butane was used to elucidate isomerization reaction mechanisms

First author, year	Catalyst	Conversion	Temp / K	Reactant	Balance gas	Reactor type
Adeeva, 1994	Fe,MnSZ	-Estimate 60 %	353	Commercial, 7 torr	14 torr Ar	Recirculation
Adeeva, 1995	SZ	~40 %, 1 h	403	Commercial, 30 torr		Recirculation
Adeeva, 1997	A	35 %, 10 min	498	Commercial, 9 torr	40 torr H_2	Recirculation
Adeeva, 1997	B	25 %, 15 min	348	Commercial, 9 torr	40 torr H_2	Recirculation
Adeeva, 1997	C	32 %, 10 min	498	Commercial, 9 torr	40 torr H_2	Recirculation
Adeeva, 1997	D	10 %, 60 min	538	Commercial, 9 torr	40 torr H_2	Recirculation
Bearez, 1985	HMOR	With time	Not given	Homemade, 0.01 bar	P = atm, unspecified bal gas	Recirculation
Garin, 1995	SZ	8-17 %	523	Homemade, 5 ul pulse	H_2	Flow
Garin, 1995	Pt/SZ	9 %	523	Homemade, 5 ul pulse	H_2	Flow
Liu, 1995	Pt/SZ	30 min	523	Commercial, 1 torr	50 torr H_2	Recirculation
Suzuki, 2001	Heteropoly, SZ, with & without Pt	Range	423-523	Commercial, 40 torr	200 torr H_2	Recirculation
Suzuki, 2004	Heteropoly, with & without Pt	Range	393-623	Commercial, 40 torr	200 torr H_2	Recirculation

Scheme 1

1. $n\text{-}C_4H_{10}\,(g) \rightleftharpoons n\text{-}C_4H_8\,(g) + H_2\,(g)$
2. $n\text{-}C_4H_8\,(g) + Z^-H^+ \rightleftharpoons n\text{-}C_4H_9 \cdot Z$
3. $n\text{-}C_4H_9 \cdot Z \rightarrow i\text{-}C_4H_9 \cdot Z$
4. $i\text{-}C_4H_9 \cdot Z \rightleftharpoons i\text{-}C_4H_8\,(g) + Z^-H^+$
5. $i\text{-}C_4H_8\,(g) + H_2 \rightleftharpoons i\text{-}C_4H_{10}\,(g)$
6. $i\text{-}C_4H_9 \cdot Z + n\text{-}C_4H_{10}\,(g) \rightleftharpoons i\text{-}C_4H_{10}\,(g) + n\text{-}C_4H_9 \cdot Z$

Scheme 1: Individual reactions involved in the monomolecular isomerization pathway assuming that methyl-shift (Step 3) is rate-limiting.

Scheme 2

1. $n\text{-}C_4H_{10}\,(g) \rightleftharpoons n\text{-}C_4H_8 + H_2\,(g)$
2. $n\text{-}C_4H_8\,(g) + Z^-H^+ \rightleftharpoons n\text{-}C_4H_9 \cdot Z$
3. $n\text{-}C_4H_9 \cdot Z + n\text{-}C_4H_8\,(g) \rightleftharpoons C_8H_{17} \cdot Z$
4. $C_8H_{17} \cdot Z \rightleftharpoons i\text{-}C_8H_{17} \cdot Z$
5. $i\text{-}C_8H_{17} \cdot Z \rightarrow C_3H_6\,(g) + i\text{-}C_5H_{11} \cdot Z$
6. $C_3H_6\,(g) + H_2\,(g) \rightleftharpoons C_3H_8\,(g)$
7. $i\text{-}C_5H_{11} \cdot Z + n\text{-}C_4H_{10} \rightleftharpoons i\text{-}C_5H_{12} + n\text{-}C_4H_9 \cdot Z$

Scheme 2: Individual reactions involved in the bimolecular disproportionation pathway assuming that beta-scission (Step 5) is rate-limiting.

Scheme 3

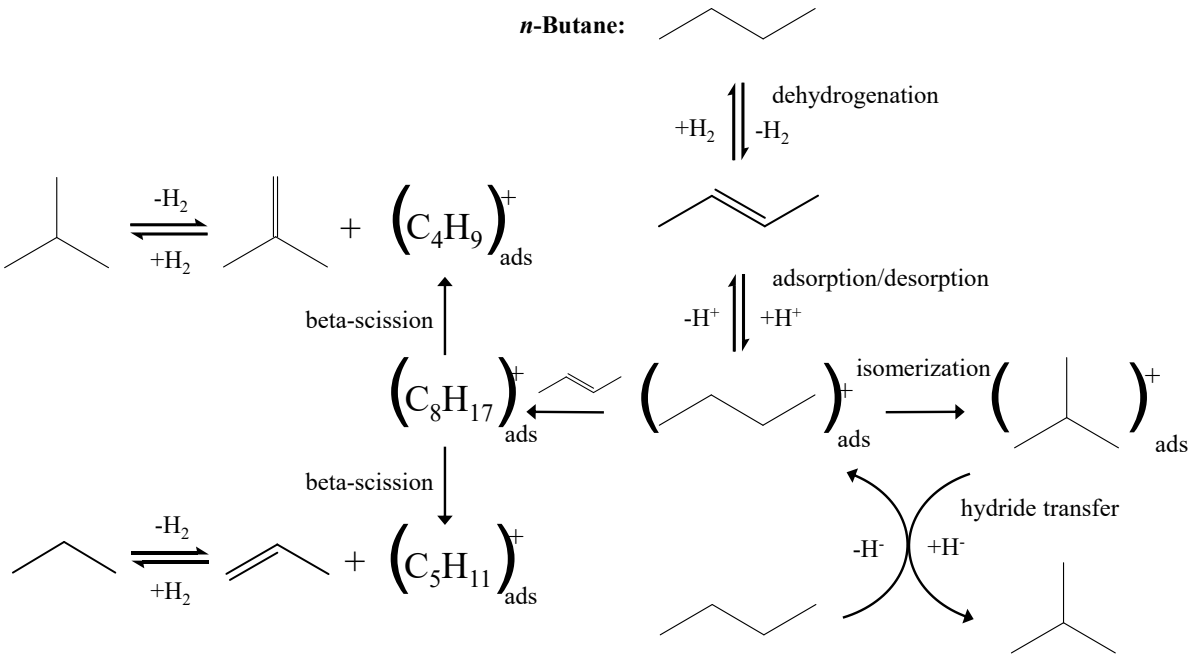

Scheme 3: Possible reaction pathways of *n*-butane on Pt/H-mordenite.